Application of the Fröbenius method to the Schrödinger equation for a spherically symmetric potential: an anharmonic oscillator

2005 J. Phys. A: Math. Gen. 38 7743

(http://iopscience.iop.org/0305-4470/38/35/008)

INSTITUTE OF PHYSICS PUBLISHING JOURNAL OF PHYSICS A: MATHEMATICAL AND GENERAL

J. Phys. A: Math. Gen. **38** (2005) 7743–7755 doi:10.1088/0305-4470/38/35/008

Application of the Fröbenius method to the Schrödinger equation for a spherically symmetric potential: an anharmonic oscillator

Przemysław Kościk and Anna Okopińska

Institute of Physics, Świętokrzyska Academy ul. Świętokrzyska 15, 25-406 Kielce, Poland

Received 23 May 2005
Published 16 August 2005
Online at stacks.iop.org/JPhysA/38/7743

Abstract

The power series method has been adapted to compute the spectrum of the Schrödinger equation for central potential of the form $V(r) = \frac{d_{-2}}{r^2} + \frac{d_{-1}}{r} + \sum_{i=0}^{\infty} d_i r^i$. The bound-state energies are given as zeros of a calculable function, if the potential is confined in a spherical box. For an unconfined potential the interval bounding the energy eigenvalues can be determined in a similar way with an arbitrarily chosen precision. The very accurate results for various spherically symmetric anharmonic potentials are presented.

PACS number: 03.65.Ge

(Some figures in this article are in colour only in the electronic version)

1. Introduction

The exact solution of the Schrödinger equation can be obtained only for a few particular forms of potentials, in other cases one has to resort to approximations or numerical techniques. Many approximation methods have been developed for solving problems in one-dimensional space. Approximate solutions to the Schrödinger equation have also been studied for spherically symmetric potentials in D-dimensional space, both by methods elaborated for one-dimensional space, e.g., the Hill determinant method [1], the variational approach [2], and by methods dedicated to D-dimensional problems, e.g., the shifted $1/D$ expansion [3, 4]. Here we show that highly accurate solutions to the Schrödinger equation can be determined for various types of spherically symmetric potentials with the use of the Fröbenius method (FM). The method consists in expanding the solution of a differential equation into power series [5], and was originally applied by Barakat and Rosner [6] to compute the spectrum of a one-dimensional quartic oscillator confined by impenetrable walls at $x = \pm R$. The energy eigenvalues of the system have been obtained numerically as zeros of a function, calculated from its power series representation. Moreover, it has been shown that the bound-state energies of the confined system approach rapidly those of the unconfined oscillator for increasing R.

Low-lying eigenvalues for other one-dimensional potentials [7] have also been successfully calculated in a similar way. Recently, a modified treatment of unconfined systems allowed for a very accurate determination of the ground-state energy for the quartic oscillator [8]. In all the cases studied the potential was a finite function, and a solution was expanded around an ordinary point of the differential equation. Here we study the application of the FM for solving the radial Schrödinger equation, which requires that an expansion around a regular singular point be used.

The outline of the present work is as follows. In section 2 the solution of the radial Schrödinger equation in the form of a generalized power series is discussed. The case of a spherically symmetric potential bounded by an impenetrable wall at $r = R$ is studied in section 3. In this case, the energy eigenvalues can be easily determined by finding the roots of the polynomial, which is illustrated in the example of the confined harmonic and anharmonic oscillators and Hulthén potential. The case of an unconfined system is studied in section 4, where a scheme for determining an arbitrarily large set of bound-state energies is developed. After demonstrating the performance of the method in the exactly solvable example of the Kratzer potential, the results for the unconfined oscillator are presented for various choices of anharmonic parameters.

2. Expansion around a regular singular point

The Schrödinger equation for a spherically symmetric potential in three-dimensional space can be reduced to an ordinary differential equation in the radial variable

$$\left[-\frac{1}{2r}\frac{\mathrm{d}^2}{\mathrm{d}r^2}r + \frac{l(l+1)}{2r^2} + V(r)\right] R(r) = \lambda R(r), \tag{1}$$

where l is the angular momentum quantum number, and the units $\hbar = 1, m = 1$ are used. Upon introducing the function $u(r) = rR(r)$, the differential equation (1) takes the form of the one-dimensional Schrödinger eigenvalue problem

$$\left[-\frac{1}{2}\frac{\mathrm{d}^2}{\mathrm{d}r^2} + V_{\mathrm{eff}}(r, l)\right] u(r) = \lambda u(r), \tag{2}$$

where the effective potential reads

$$V_{\mathrm{eff}}(r, l) = \frac{l(l+1)}{2r^2} + V(r). \tag{3}$$

The point $r = 0$ is a regular singular point of the radial equation, if the potential $V(r)$ diverges but $r^2V(r)$ remains finite as $r \to 0$, which is the case for the interaction potential of the form

$$V(r) = \frac{d_{-2}}{r^2} + \frac{d_{-1}}{r} + V_{\mathrm{reg}}(r), \tag{4}$$

where the regular part is represented by a convergent series

$$V_{\mathrm{reg}}(r) = \sum_{i=0}^{\infty} d_i r^i. \tag{5}$$

In this case, the FM can be applied with the radial wavefunction represented as a generalized power series

$$u(r) = r^{\delta} \sum_{i=0}^{\infty} a_i r^i, \tag{6}$$

where $a_0 \neq 0$. In what follows, we will take $a_0 = 1$, since normalization of the wavefunction is irrelevant in our calculation. Substituting (6) into (2) we obtain the equation

$$-\frac{1}{2}\sum_{i=0}^{\infty}[(i+\delta)(i+\delta-1)-l(l+1)]a_i r^i + \left(\sum_{i=0}^{\infty} d_{i-2} r^i\right)\left(\sum_{i=0}^{\infty} a_i r^i\right) = \lambda \sum_{i=0}^{\infty} a_i r^{i+2}, \tag{7}$$

which, by comparing the coefficients of like powers of r, yields the recurrence relation

$$[(i+\delta)(i+\delta-1)-l(l+1)]a_i - 2\sum_{n=0}^{i} d_{i-2-n}a_n + 2a_{i-2}\lambda = 0, \tag{8}$$

where $a_i = 0$ for $i < 0$. Setting $i = 0$ in the above relation, we obtain the indicial equation

$$[\delta(\delta-1)-l(l+1)-2d_{-2}]a_0 = 0, \tag{9}$$

which is solved by

$$\delta_1 = \tfrac{1}{2}\left(1-\sqrt{8d_{-2}+(1+2l)^2}\right), \qquad \delta_2 = \tfrac{1}{2}\left(1+\sqrt{8d_{-2}+(1+2l)^2}\right). \tag{10}$$

The Fuchs's theorem [5] asserts that the generalized series (6) converges, and both linearly independent solutions of the Schrödinger equation (2) are obtained as generalized series, one with $\delta = \delta_1$ and the other with $\delta = \delta_2$ (except the special case when $\delta_2 - \delta_1 = \sqrt{8d_{-2}+(1+2l)^2}$ is equal to a non-negative integer). The value of δ determines the behaviour of $u(r)$ for $r \to 0$, and only $\delta > \frac{1}{2}$ is acceptable [9], since only in this case the mean value of the kinetic energy is finite. Such a solution to the Schrödinger equation (2) exists only if the potential is such that $d_{-2} > -\frac{1}{8}$. This solution contains only the series with $\delta = \delta_2$, and in the following will be denoted by

$$u(r,\lambda) = r^{\delta_2}\sum_{i=0}^{\infty} a_i r^i, \tag{11}$$

where the dependence on the energy eigenvalue λ is explicitly marked. The coefficients of the series are determined recurrently as

$$a_i = \frac{-2\lambda a_{i-2} + 2\sum_{n=0}^{i-1} d_{i-2-n}a_n}{i\left(i+\sqrt{8d_{-2}+(1+2l)^2}\right)}. \tag{12}$$

The function $u(r,\lambda)$ has an important property that $u(0,\lambda) = 0$, which can be regarded as a boundary condition for the radial equation at $r = 0$. The second boundary condition should be chosen according to the physical bounds in the investigated problem.

3. Confined potentials

The simplest scheme arises in the case of radially symmetric potential $V(r)$ additionally bounded by an infinitely high wall at $r = R$. In this case, the second boundary condition for a particle with angular momentum l is of the form

$$u(R,\lambda) = 0, \tag{13}$$

yielding an exact quantization condition that gives the bound-state energies as zeros of a calculable function. The values of λ, determined from the above condition, are denoted by λ_{nl}, where $n = 0, 1, \ldots$ counts the number of zeros in the radial variable in the Sturm–Liouville eigenvalue problem [10]. In the numerical calculation, the function $u(R,\lambda)$ has to be approximated by truncating the series in (11) at suitably high-order K, which can be done with an arbitrary accuracy, as the series is convergent. The truncated function is a polynomial

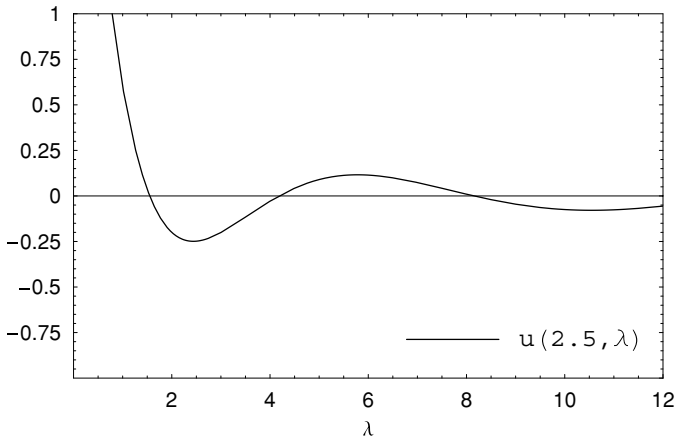

Figure 1. Behaviour of $u(R, \lambda)$ for the spherically symmetric harmonic oscillator with $\omega = 1$ and $l = 0$ at $R = 2.5$.

of degree K in the variable λ, that can be used to advantage in determining the numerical values of its zeros. In this way, an increasing amount of bound-state energies can be obtained with increasing accuracy as the truncation order $K \to \infty$. Considering the growing interest in quantum confined systems, the method (and its possible modifications for different symmetries of the confining box) can find application in the studies of semiconductor nanostructures such as quantum dots [11–13]. Here we consider a few examples.

3.1. The harmonic oscillator

The performance of the FM will be demonstrated for the spherical harmonic oscillator

$$V(r) = \frac{\omega^2}{2} r^2, \tag{14}$$

enclosed by a sphere of radius R. The typical behaviour of $u(R, \lambda)$ as a function of λ is shown in figure 1 in the example of the oscillator with $\omega = 1$ for $l = 0$ and $R = 2.5$. The approximate $u(R, \lambda)$ is a polynomial in λ and the truncation affects only its behaviour for large λ. We determine thus the bound-state energies as roots of the obtained polynomial with the use of the NSolve procedure from the Mathematica package, without any need for introducing starting values for λ. The stability of the numerical results was achieved by increasing the number of non-vanishing terms K until the values of $\lambda_{nl}(R)$, corresponding to the states (n, l) of angular momentum l, become stable to the desired accuracy. The values of $\lambda_{nl}(R)$, obtained for the harmonic oscillator of frequency $\omega = 1$, are compared in table 1 with the eigenvalues of the unconfined oscillator, $E_{nl} = 2n + l + \frac{3}{2}$. In figure 2 the low-lying state energies are plotted as a function of the confinement radius R. One can observe how the non-degenerate levels of the confined system approach the equidistant states of the unconfined oscillator, as the radius of enclosure grows.

3.2. The anharmonic oscillator

The quantum anharmonic oscillator is widely used for describing the physical phenomena, especially in the condensed matter and molecular physics. However, the case of a confined

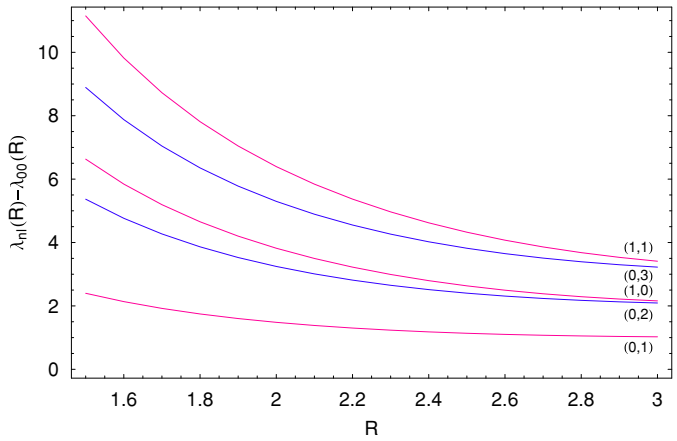

Figure 2. Behaviour of $\lambda_{nl}(R) - \lambda_{00}(R)$ for the harmonic oscillator as a function of the confinement radius R.

Table 1. The low-lying energy levels of the harmonic oscillator with $\omega = 1$ confined at various R.

l	n	$\lambda_{nl}(1.5)$	$\lambda_{nl}(2.5)$	$\lambda_{nl}(3)$	$\lambda_{nl}(3.5)$	$\lambda_{nl}(4)$	E_{nl}
0	0	2.504 9762	1.551 4217	1.506 0815	1.500 3995	1.500 0146	1.5
1	0	4.903 5904	2.688 1440	2.531 2925	2.502 9102	2.500 1438	2.5
0	1	9.135 4221	4.184 2613	3.664 2196	3.523 3023	3.501 6915	3.5
2	0	7.871 7305	3.953 5289	3.598 2477	3.512 5803	3.500 8421	3.5

anharmonic system has been discussed only for the one-dimensional example [6]. Here we study the spherically symmetric anharmonic oscillator with a potential of the form

$$V_{\mathrm{AO}}(r) = \frac{\omega^2}{2} r^2 + g r^{2J} \tag{15}$$

for different values of the power J. The analysis can be simplified by using the rescaled variables

$$\widehat{r} = g^{-\frac{1}{2J+2}} r, \qquad \text{and} \qquad \widehat{\lambda} = \lambda g^{-\frac{2}{2J+2}}$$

then equation (2) takes the form

$$\left[-\frac{1}{2} \frac{\mathrm{d}^2}{\mathrm{d}\widehat{r}^2} + \frac{l(l+1)}{2\widehat{r}^2} + V_{\mathrm{AO}}(\widehat{r}) \right] u(\widehat{r}) = \widehat{\lambda} u(\widehat{r}), \tag{16}$$

where

$$V_{\mathrm{AO}}(\widehat{r}) = z\widehat{r}^2 + \widehat{r}^{2J} \tag{17}$$

depends on the dimensionless parameter

$$z = \frac{\omega^2}{2} g^{-\frac{4}{2J+2}}, \tag{18}$$

which accounts for a relative strength of the harmonicity and anharmonicity. In the following, we skip the hats over r and λ. We consider the solution of (16), which is regular at $r = 0$, as given by the generalized power series

$$u(r, \lambda) = r^{l+1} \sum_{i=0}^{\infty} a_i r^{2i} \tag{19}$$

Table 2. The bound-state energies $\lambda_{nl}(R)$ of the confined anharmonic oscillator.

l	n	z	$\lambda_{nl}(0.5)$	$\lambda_{nl}(1)$	$\lambda_{nl}(1.5)$	$\lambda_{nl}(2)$	$\lambda_{nl}(2.5)$
0	0	5	20.098 750 27	6.392 918 17	5.108 642 45	5.069 740 45	5.069 663 68
		4	20.028 406 81	6.132 287 81	4.691 291 08	4.633 484 73	4.633 308 31
		3	19.957 993 89	5.867 539 35	4.247 150 28	4.160 267 90	4.159 847 13
		−1	19.675 646 22	4.765 921 59	2.126 682 80	1.633 225 95	1.612 781 77
		−3	19.534 053 95	4.188 602 46	0.804 479 58	−0.383 942 86	−0.540 591 17
1	0	5	40.859 898 45	12.087 751 01	8.802 120 12	8.637 447 01	8.636 883 71
		4	40.766 487 91	11.730 352 16	8.164 580 83	7.939 507 15	7.938 336 01
		3	40.673 026 07	11.369 722 35	7.498 294 58	7.189 633 53	7.187 145 92
		−1	40.298 665 54	9.894 682 26	4.512 452 22	3.406 939 67	3.347 395 53
		−3	40.111 177 31	9.137 546 42	2.810 772 29	0.782 858 38	0.504 133 22

with the recurrence relation of the form

$$a_i = \frac{-2\lambda a_{i-1} + 2z a_{i-2} + 2a_{i-(J+1)}}{2i(1+2i+2l)}, \tag{20}$$

where $a_0 = 1$. In the case of the oscillator enclosed by a sphere of radius R the bound-state energies are easily determined as zeros of $u(R, \lambda)$. In table 2 the numerical results are presented in the example of the quartic oscillator ($J = 2$) with different values of parameter z and for different radii of enclosure R. The spectrum of an unconfined anharmonic oscillator will be studied in the next section.

3.3. Hulthén potential

The FM can also be useful for computing energy eigenvalues, in the case when the series expansion of its regular part (5) converges only in a finite interval ρ_V. In this case, the convergence of the generalized series solution (11) is granted only for $r < \rho_V$ and the problem is well defined only for the confinement radius $R < \rho_V$. If the confining box projects beyond the convergence sphere, we must be very careful, since for $r > \rho_V$ the series representation $u(r, \lambda)$ does not necessarily coincide with the solution of the radial Schrödinger equation in the potential $V(r)$. As an example, we consider the Hulthén potential

$$V(r) = \frac{-\delta\, \mathrm{e}^{-\delta r}}{1 - \mathrm{e}^{-\delta r}}, \tag{21}$$

when the screening parameter $\delta > 0$ is not too large. To employ the FM we expand the Hulthén potential into the Laurent series

$$V(r) = -\frac{1}{r} + V_{\mathrm{reg}}(r), \tag{22}$$

with the regular part given by

$$V_{\mathrm{reg}}(r) = \frac{\delta}{2} - \delta \sum_{n=0}^{\infty} g_n [\delta r]^{2n+1}, \tag{23}$$

where

$$g_n = \frac{(-1)^n \beta_{n+1}}{[2(n+1)]!}, \tag{24}$$

Table 3. Bound-state energies of the Hulthén potential for various values of the radius of confinement R.

l	$n = n_r$	δ	$\lambda_{nl}(4)$	$\lambda_{nl}(6)$	$\lambda_{nl}(8)$	$\lambda_{nl}(12)$	E_{nl}
0	0	0.050	−0.458 5448	−0.475 2873	−0.475 3117	−0.475 3125	−0.475 3125
		0.075	−0.446 3941	−0.463 1776	−0.463 2024	−0.463 2031	−0.463 2031
0	1	0.050	0.444 7886	−0.060 6327	−0.088 8523	−0.097 5630	−0.101 2500
		0.075	0.456 7303	−0.049 2481	−0.077 6572	−0.086 4942	−0.090 3125
1	0	0.050	0.168 0730	−0.080 2458	−0.094 7675	−0.099 2341	−0.101 0425
		0.075	0.180 0057	−0.068 7394	−0.083 4014	−0.087 9576	−0.089 8478

and β_n are given [14] by a convenient expression

$$\beta_n = (-1)^n \frac{n}{2^{2n}-1} \sum_{k=1}^{2n-1} \frac{1}{2^k} \sum_{j=1}^{k} (-1)^j \binom{k}{j} j^{2n-1}. \tag{25}$$

The convergence radius of (23) is $\rho_V = \frac{2\pi}{\delta}$, and in the range $0 \leqslant r < \rho_V$ the potential (22) can be approximated with an arbitrary accuracy by a series with a finite number of terms. With the series truncated after the r^{2P+1} term, the recursion relation (12) takes the form

$$a_i = \frac{-2a_{i-1} + 2\left(\frac{\delta}{2} - \lambda\right)a_{i-2} - 2\sum_{j=1}^{P+1} \delta^{2j} g_{j-1} a_{i-(2j+1)}}{i(i+2l+1)}. \tag{26}$$

In table 3 the numerical results are presented for different values of δ at various radii of enclosure $R < \rho_V$. Numerical stability was achieved by increasing the number of terms both in the series solution (11) and in the potential expansion (23) until the approximate values λ_{nl} for fixed R become stable to the quoted accuracy. The table also contains the exact eigenvalues E_{nl} for the unconfined Hulthén potential, obtained analytically ($l = 0$) and by numerical integration ($l \neq 0$) [15].

4. Unconfined potentials

Now we come to the discussion of unconfined potentials, namely to the case of a particle with the angular momentum l in a spherically symmetric potential of the form (4) without any external enclosure. An unconfined system can also be effectively treated by the FM, as demonstrated by the calculation of the ground-state energy of the one-dimensional anharmonic oscillator to a very high precision of 1184-digits [8]. Here we show that the method can be implemented in a way that also allows for computing the excited state energies. We take the generalized series (11), as a solution of the radial Schrödinger equation, which fulfils the boundary condition $u(\lambda, 0) = 0$, and consider two ways of imposing the second boundary condition at finite $r = R$, namely $u(R, \lambda) = 0$ or $u^{(1)}(R, \lambda) = 0$. At $R \to \infty$ both conditions are satisfied at the same values of λ, which correspond to the energy eigenvalues E_{nl} of the unconfined system, where $n = 0, 1, 2, \ldots$. At finite R the values of λ are different: let us denote by λ_{kl} the values satisfying

$$u(R, \lambda_{kl}) = 0 \qquad \text{for} \quad k = 0, 1, \ldots, \tag{27}$$

and by λ'_{kl} those satisfying

$$u^{(1)}(R, \lambda'_{kl}) = 0, \qquad \text{for} \quad k = 0, 1, \ldots. \tag{28}$$

In both cases we deal with the Sturm–Liouville eigenvalue problem; the nodes of the function $u(r, \lambda_{kl})$ in the radial variable divide thus the domain $(0, R)$ precisely into k-parts [10], and

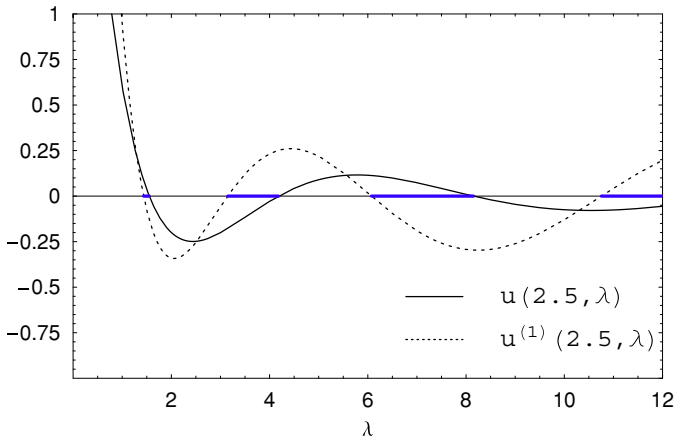

Figure 3. Behaviour of $u(R,\lambda)$ (the solid line) and $u^{(1)}(R,\lambda)$ (the dashed line) for the spherically symmetric harmonic oscillator with $\omega = 1$ and $l = 0$ at $R = 2.5$. The three first bounding intervals are marked by a thick line.

the same is true for the function $u(r,\lambda'_{kl})$. The energy eigenvalues satisfy thus the following inequalities:

$$\lambda'_{0l} < \lambda_{0l} < \lambda'_{1l} < \lambda_{1l} < \lambda'_{2l} < \lambda_{2l} < \cdots < \lambda'_{kl} < \lambda_{kl} < \cdots. \tag{29}$$

It is easy to check that the sign of $u(R,\lambda)$ is opposite to that of $u^{(1)}(R,\lambda)$, for any value λ lying within $(\lambda'_{kl},\lambda_{kl})$, which will be called the bounding interval in the following. Whereas, for values of λ in the interval $(\lambda_{kl},\lambda'_{k+1l})$ the signs of $u(R,\lambda)$ and $u^{(1)}(R,\lambda)$ are the same. These properties are best illustrated in figure 3, in the example of $u(r,\lambda)$ calculated for the spherical harmonic oscillator with angular momentum $l = 0$.

Bound states in the radial potential $V(r)$ are possible only for $\lambda < \lim_{r\to\infty} V(r)$. In this case, there exists a point R_c such that for $r > R_c$ we have $V_{\text{eff}}(r,l) - \lambda > 0$ and the sign of $u^{(2)}(r,\lambda)$ is the same as that of $u(r,\lambda)$, which implies that for $r > R_c$ the function $u(r,\lambda)$ must neither have a local maximum if $u(R_c,\lambda) > 0$, nor a local minimum if $u(R_c,\lambda) < 0$. If both $u(R_c,\lambda)$ and $u^{(1)}(R_c,\lambda)$ are positive (negative), then $u(r,\lambda)$ and $u^{(1)}(r,\lambda)$ tend monotonically to the plus (minus) infinity. Therefore, if the point of imposing the boundary condition R is larger than R_c, the following inequality is satisfied,

$$\lambda'_{0l} < E_{0l} < \lambda_{0l} < \cdots < \lambda'_{kl} < E_{kl} < \lambda_{kl} < \cdots < \lambda'_{nl} < E_{nl} < \lambda_{nl}, \tag{30}$$

where $\lambda_{nl} < V_{\text{eff}}(R,l)$. For increasing R, the energy $\lambda'_{kl}(R)$ grows and $\lambda_{kl}(R)$ decreases, approaching the exact eigenvalue E_{kl} from both sides monotonically. This allows for bounding the energy eigenvalues of an unconfined system with a required precision. With the approximate $u(R,\lambda)$, obtained by truncating the number of terms in the generalized power series to K, both (27) and (28) are polynomial equations in λ. The large set of energy levels can thus be determined numerically by finding the roots of polynomials. Generally, the bounding intervals are larger for higher states but for increasing R all the bounding intervals shrink. We determine thus the new bounding intervals with the value of R increased by a suitably chosen ΔR. The iteration procedure is repeated for $R_i = R + i\Delta R$, until the bounding energies for a chosen state (k,l) become equal to the accuracy desired, which determines its energy with that accuracy. If the procedure does not converge for the state of interest, the number of terms K, which are included in the power series (11) should be increased.

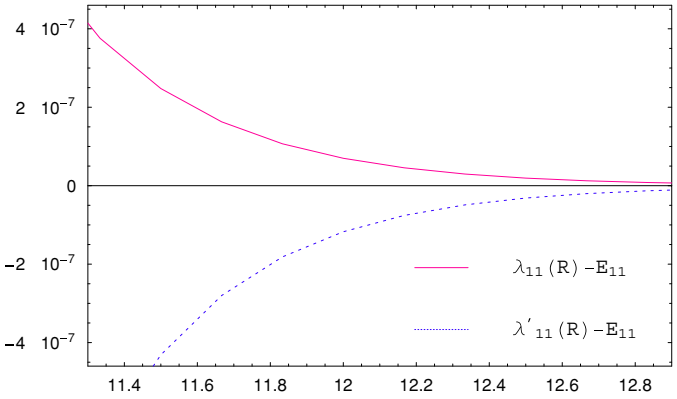

Figure 4. Convergence of $\lambda_{11}(R) - E_{11}$ and $\lambda'_{11}(R) - E_{11}$ to zero, demonstrated as a function of R.

Table 4. Comparison of the convergence of $\lambda_{11}(R)$ and $\lambda'_{11}(R)$ to the exact value $E_{11} = -1.4476568219254$ for different values of R and ΔR.

i	R	ΔR	$\lambda_{11}(R_i)$	$\lambda'_{11}(R_i)$
0	5	0.5	−1.3178526137388	−1.8092879070838
1			−1.3839260262988	−1.6834926644347
2			−1.4178923369387	−1.5810678698537
3			−1.4345142511694	−1.5094745737014
0	8	1	−1.4468612319721	−1.4500438665400
1			−1.4475622942994	−1.4478789515475
2			−1.4476472391241	−1.4476761151204
3			−1.4476559628487	−1.4476583796562
0	14	2	−1.4476568215565	−1.4476568224842
1			−1.4476568219238	−1.4476568219276
2			−1.4476568219254	−1.4476568219254

4.1. The Kratzer potential

For demonstrating the convergence of the algorithm previously formulated, we first consider the Schrödinger problem in the Kratzer potential

$$V(r) = \frac{d_{-2}}{r^2} + \frac{d_{-1}}{r}, \tag{31}$$

for which the exact energy levels are given by

$$E_{nl} = -2d_{-1}^2\left(2n + 1 + \sqrt{(2l+1)^2 + 8d_{-2}}\right)^{-2}, \qquad (n = 0, 1, 2, \ldots). \tag{32}$$

Choosing $d_{-1} = -8$ and $d_{-2} = 4$ as the parameters of the potential (31), we carry out the calculation for the state (1, 1), taking the number of terms in the power series (11) suitably large ($K = 160$) in order to assure the numerical stability. Table 4 shows with 14-digit precision the values of $\lambda_{11}(R_i)$, obtained from the condition (27), and those of $\lambda'_{11}(R_i)$, obtained from (28), for $R_i = R + i\Delta R$. The bounding interval shrinks very fast and the exact value of energy is easily determined with 14-digit precision, $E_{11} = -1.447\,656\,821\,9254$. Figure 4 shows how the deviations from the exact energy monotonically diminish for increasing R, the energy difference $\lambda_{11}(R) - E_{11}$ approaches zero from above, and $\lambda'_{11}(R) - E_{11}$ from below.

Table 5. The lowest bound-state energies of the quartic oscillator for negative values of z.

z	E_{00}	E_{01}	E_{02}	E_{03}	E_{04}
−10	−21.889 658 23	−21.667 599 59	−21.227 751 92	−20.577 769 33	−19.727 423 47
−9	−17.308 115 08	−17.056 343 13	−16.560 062 80	−15.831 552 72	−14.885 436 07
−8	−13.237 578 18	−12.946 304 09	−12.377 237 45	−11.550 865 71	−10.489 174 35
−7	−9.680 640 55	−9.334 032 78	−8.668 660 23	−7.719 398 51	−6.518 583 69
−6	−6.640 628 24	−6.211 333 59	−5.416 359 74	−4.313 404 68	−2.947 175 08

4.2. The anharmonic oscillator

The unconfined quantum anharmonic oscillator is one of the most frequently discussed quantum systems. Especially the one-dimensional example, being the simplest tractable model of quantum field theory [16], is routinely used for examining the validity of various approximation methods [17], as its exact solution can be numerically determined to an arbitrary accuracy [8, 18–20]. The D-dimensional case is much less studied; generally, a spherically symmetric anharmonic potential (15) for different values of the anharmonicity power J is discussed. The quartic potential ($J = 2$) was studied by means of various approximation methods, e.g., the self-similar approximation [21], the random phase approximation [22] and the artificial perturbation method [23]. There are also a few reports in the literature of the numerically exact results for the quartic [18, 24, 25], sextic ($J = 3$) [1, 24] and octic ($J = 4$) potential [24] in the limited range of the anharmonicity parameter z.

Here we show that the FM enables us to determine effectively the spectrum of the unconfined spherical anharmonic oscillator (15) in the wide range of parameter z. With the solution of the Schrödinger equation $u(r, \lambda)$ in the form of the generalized series (19) we determine the numerical values of bound-state energies, using the procedure formulated in the beginning of this section. After checking that the results available in the literature [1, 24, 25] are easily recovered to the quoted accuracy, we performed an extensive calculation of the spectrum of spherically symmetric anharmonic oscillators. The highly accurate results presented here may serve for testing the quality of various approximation methods. An especially challenging test is provided by the data obtained for negative values of parameter z, when the anharmonic potential has a Mexican hat shape. This range was not explored before, and the numerical data for bound-state energies were lacking. Therefore, in table 5 we present our results for several lowest state (n, l) energies of the quartic oscillator ($J = 2$) at negative values of z. In table 6 we compare the bound-state energies for oscillators with different anharmonicity powers ($J = 2, 3, 4$) at various values of z. The results up to 8-decimal precision are quoted, but it is not difficult to improve the accuracy at will. However, one has to note that the effort of the calculation increases for higher states. The appropriate shrinking of the intervals bounding the higher states energies is achieved only at large R, which requires the larger number of terms K to be included in the power series. The computational effort increases strongly, when the parameter z becomes more negative, i.e., for increasing radius of the hat. For example, equality of the values $\lambda_{00}(R)$ and $\lambda'_{00}(R)$ with 8-digit accuracy was achieved for $z = -2$ at the radius $R = 3$, which requires $K = 65$, while for $z = -10$ the same is obtained only at $R = 3.9$, which requires $K = 140$.

Our results for the quartic oscillator are presented graphically in figure 5. The excitation energies with respect to the ground state, $E_{nl} - E_{00}$, are plotted as a function of parameter z, which covers the range $-15 < z < 25$. The values of $z < 0$ correspond to the Mexican hat, and those of $z > 0$ to the single-well shape of the anharmonic potential (17). It is interesting

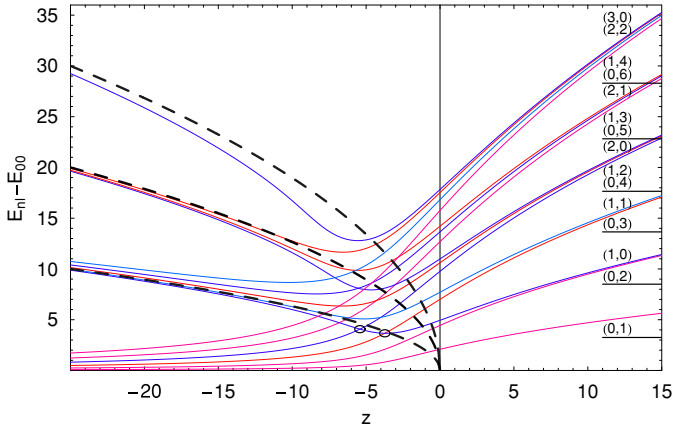

Figure 5. The behaviour $E_{nl} - E_{00}$ as a function of z, the asymptotic behaviour of $E_n - E_0 = n\sqrt{-4z}$ is shown by dashed lines. Two points of level crossing are marked by circles.

Table 6. The low-lying eigenvalues of anharmonic oscillators for certain powers of anharmonicity $2J$ at different values of parameter z.

J	z	E_{00}	E_{01}	E_{02}	E_{10}	E_{03}
2	−5	−4.119 111 33	−3.559 581 00	−2.591 375 76	−0.210 676 02	−1.300 274 63
	−4	−2.103 494 62	−1.341 758 38	−0.151 623 31	1.573 350 20	1.360 987 87
	−3	−0.542 125 26	0.500 947 41	1.955 808 51	3.177 122 98	3.716 716 98
	−2	0.661 428 90	2.040 645 01	3.787 797 23	4.665 390 82	5.813 954 33
	0.1	2.464 636 53	4.583 218 26	6.965 292 41	7.458 911 76	9.563 146 73
	0.5	2.737 892 27	4.991 430 53	7.491 775 05	7.942 403 98	10.197 048 22
	1	3.057 945 73	5.475 919 99	8.121 714 27	8.526 737 39	10.959 728 25
	2	3.639 482 05	6.371 630 94	9.299 405 83	9.633 627 91	12.396 872 79
	5	5.069 663 67	8.636 883 66	12.336 855 80	12.550 115 13	16.158 439 62
	8	6.217 225 63	10.494 777 25	14.870 645 91	15.024 541 65	19.339 216 39
3	−8	−5.009 826 91	−4.085 816 39	−2.499 273 39	1.270 195 37	−0.376 121 49
	−5	−1.398 616 13	−0.060 702 41	1.931 236 53	4.231 923 90	4.436 291 85
	−2	1.241 449 88	3.208 456 49	5.723 568 78	7.058 032 62	8.686 894 46
	−1	1.945 044 86	4.152 385 70	6.860 552 53	7.977 455 78	9.989 547 03
	0.1	2.639 852 66	5.118 530 12	8.045 438 12	8.969 778 43	11.361 855 73
	1	3.156 300 57	5.858 368 53	8.967 280 95	9.763 935 91	12.440 024 44
4	−8	−3.207 120 29	−1.834 342 72	0.369 155 24	4.031 708 82	3.245 222 74
	−5	−0.572 392 28	1.199 307 11	3.749 325 88	6.246 321 14	6.932 073 43
	−2	1.555 757 37	3.855 870 69	6.823 256 01	8.475 000 53	10.358 574 48
	−1	2.165 259 09	4.662 764 45	7.782 509 48	9.219 184 47	11.444 451 27
	0.1	2.785 948 28	5.508 217 86	8.801 597 88	10.034 954 45	12.607 376 64
	1	3.258 870 03	6.168 872 93	9.608 194 32	10.698 253 37	13.534 823 09
5	0.1	2.911 881 67	5.817 478 81	9.380 319 19	10.834 778 15	13.544 224 29
	1	3.356 014 45	6.429 098 65	10.118 304 92	11.423 420 67	14.384 327 80

to note that, in spite of this difference, the dependence of excitation energies on z is smooth at the point separating the two cases, $z = 0$, which corresponds to the strong coupling limit, $g \to \infty$. Instead, the behaviour of excitation energies in the weak coupling limit ($|z| \to \infty$)

is very different for positive and negative z. For $z \to \infty$ we recover the radial harmonic oscillator of the frequency $2z$, energy eigenvalues of which are given by

$$E_{nl} \underset{z\to\infty}{\longrightarrow} \left(2n + l + \tfrac{3}{2}\right)\sqrt{2z}. \tag{33}$$

In figure 5 one can observe how the levels with the same $2n + l$ become degenerate for increasing z. For $z < 0$ the Mexican hat shaped anharmonic potential has a minimum at $r_{\min} = \sqrt{\frac{-z}{2}}$. If $z^3 \gg l^2$, the minimum of V_{eff} is close to $r_{\min}$ and the effective potential is approximated well by

$$V_{\text{eff}}(r) \approx -\frac{z^2}{4} + \frac{1}{2}(-4z)\left(r - \sqrt{\frac{-z}{2}}\right)^2, \tag{34}$$

which does not depend on l, and corresponds to the one-dimensional harmonic oscillator of the frequency $\sqrt{-4z}$. Therefore, in the limit $z \to -\infty$ we have

$$E_n \underset{z\to\infty}{\longrightarrow} -\frac{z^2}{4} + \left(n + \frac{1}{2}\right)\sqrt{-4z} \qquad (n = 0, 1, 2, \ldots). \tag{35}$$

In figure 5 the grouping of states with different quantum numbers l but the same value of n can be observed for strongly negative values of z. For $z \to -\infty$ all the states in the group approach the asymptotic behaviour of $E_n - E_0 = n\sqrt{-4z}$.

One can also note an interesting phenomenon of level crossing that appears in the range of $z < 0$: at a certain negative value of z two adjacent eigenvalues become degenerate. The two examples in figure 5 are marked by circles: the crossing point for the states $(1, 0)$, $(0, 3)$, which appears at $z_1 \cong -3.736\,563\,82$, and the crossing point for $(1, 0)$, $(0, 4)$, which appears at $z_2 \cong -5.420\,078\,03$. The configuration of five lowest states, which, for $z > z_1$, is given by $(0, 0)$, $(0, 1)$, $(0, 2)$, $(1, 0)$, $(0, 3)$, changes into $(0, 0)$, $(0, 1)$, $(0, 2)$, $(0, 3)$, $(1, 0)$ for $z_2 < z < z_1$, and into $(0, 0)$, $(0, 1)$, $(0, 2)$, $(0, 3)$, $(0, 4)$ for $z < z_2$. It should be stressed that in the case of the one-dimensional anharmonic oscillator the phenomenon of level crossing does not appear, this becomes possible only for systems of $D \geqslant 2$ dimensions.

5. Conclusion

We have shown that the application of the Fröbenius method to the spherically symmetrical potentials of the form $V(r) = \frac{d_{-2}}{r^2} + \frac{d_{-1}}{r} + \sum_{i=0}^{\infty} d_i r^i$ allows an easy determination of the energy spectrum. This was demonstrated first for systems enclosed in a spherical box of radius R, by studying the confined harmonic and anharmonic oscillators and Hulthén potential. With the increasing radius of confinement the bound-state energies have been shown to approach those of the corresponding unconfined systems. Even in the case of the Hulthén potential, when the convergence radius of the potential is finite, we obtain quite good approximations to the low-lying spectrum of the unconfined potential, if the screening is not too strong. Later, we developed an efficient scheme for computing eigenvalues of the Schrödinger equation for unconfined potentials with a controlled accuracy. The method allowed us to determine the low-lying state energies of spherically symmetric anharmonic oscillators with very high accuracy and moderate effort. Determination of energies becomes computationally more demanding for higher states, since more terms have to be included in the generalized power series. Our calculations cover a broad range of anharmonic parameters, both in the case of single-well potential and for the Mexican hat shape. In the latter case, the computational effort increases strongly with the increasing radius of the hat.

The method presented in this work can be easily applied for computing the precise spectrum of other spherically symmetric potentials. In the present work, we have studied the

case of three-dimensional space but the calculation of energy levels in the two-dimensional case can be performed along similar lines. The results in even and odd higher dimension D can be easily derived from those in two- and three-dimensional space, respectively, via the transformation $l \to l + \frac{D-3}{2}$. One has to add that the method can also be used to determine the approximate wavefunctions. After substituting the calculated bound-state energy to the recursion relation (12) the coefficients of the generalized series (11) can be successively determined in order to obtain the unnormalized wavefunction as a sum of the series.

References

[1] Chaudhuri R N and Mondal M 1995 *Phys. Rev.* A **52** 1850
[2] Greene R L and Aldrich C 1976 *Phys. Rev.* A **14** 2363
Lam C S and Varshni Y P 1978 *Phys. Rev.* A **19** 413
Roussel K M and O'Connel R F 1973 *Phys. Rev.* A **9** 220
Miao C-H and Qian S-W 1997 *Phys. Rev.* A **56** 2412
Stubbins C 1993 *Phys. Rev.* A **48** 220
[3] Tang A Z and Chan F T 1987 *Phys. Rev.* A **35** 911
[4] Dutt R, Mukherji U and Varshni Y P 1986 *Phys. Rev.* A **34** 777
[5] Arfken G B, Weber H J and Weber H-J 1985 *Mathematical Methods of Physicists* (Orlando, FL: Academic) pp 462–3
[6] Barakat R and Rosner R 1981 *Phys. Lett.* A **83** 149
[7] Alhendi H A and Lashin E I 2004 *Mod. Phys. Lett.* A **19** 2103 (*Preprint* quant-ph/0305128)
[8] Trott M 2000 *Preprint* quant-ph/0012147
[9] Landau L D and Lifshitz E M 1981 *Quantum Mechanics: Non-Relativistic Theory* (London: Pergamon)
[10] Courant R and Hilbert D 1989 *Methods of Mathematical Physics* (New York: Wiley-Interscience)
[11] Zhu J-L 1989 *Phys. Rev.* B **39** 8780
[12] Chuu D S, Hsiao C M and Mei N 1992 *Phys. Rev.* B **46** 3898
[13] Yang C-C, Liu L-C and Chang S-H 1998 *Phys. Rev.* B **58** 1954
[14] Schwatt I J 1924 *An Introduction to The Operations with Series* (Philadelphia)
[15] Varshni Y P 1990 *Phys. Rev.* A **41** 4682
[16] Bender C M and Wu T T 1969 *Phys. Rev.* **184** 1231
[17] Stevenson P M 1981 *Phys. Rev.* D **23** 2916
Patnaik P K 1987 *Phys. Rev.* D **35** 1234
de Deus J D 1982 *Phys. Rev.* D **26** 2782
de Saavedra F A and Buendía E 1990 *Phys. Rev.* A **42** 5073
[18] Hioe F T, MacMillen D and Montroll E W 1978 *Phys. Rep.* C **43** 305
[19] Balsa R, Plo M, Esteve J G and Pacheco A F 1983 *Phys. Rev.* D **28** 1945
Okopińska A 1987 *Phys. Rev.* D **36** 1273
[20] Gómez F J and Sesma J 2005 *J. Phys. A: Math. Gen.* **38** 3193–202
[21] Yukalova E P and Yukalov V I 1993 *J. Phys. A: Math. Gen.* **26** 2011
[22] Aouissat Z and Martin C 2004 *Eur. Phys. J.* A **19** 289
[23] Mustafa O and Odeh M 2000 *Eur. Phys. J.* B **15** 143–8
[24] Witwit M R M 1991 *J. Phys. A: Math. Gen.* **24** 4535
Witwit M R M and Gordon N A 1998 *Can. J. Phys.* **76** 609
[25] Lakshmanan M *et al* 1994 *Phys. Rev.* A **49** 3296